This is the peer reviewed version of the following article: [Andjelković, M., Tomović, L., & Ivanović, A. (2017). Morphological integration of the kinetic skull in Natrix snakes. Journal of Zoology, DOI:10.1111/jzo.12477.], which has been published in final form at [https://doi.org/10.1111/jzo.12477]. This article may be used for non-commercial purposes in accordance with Wiley Terms and Conditions for Self-Archiving.

Journal of Zoology

ZSL LET'S WORK FOR WILDLIFE

Journal of Zoology. Print ISSN 0952-8369

Morphological integration of the kinetic skull in *Natrix* snakes

M. Andjelković[1], L. Tomović[2] & A. Ivanović[2,3]

1 University of Belgrade, Institute for Biological Research "Siniša Stanković", Belgrade, Serbia
2 University of Belgrade, Faculty of Biology, Belgrade, Serbia
3 Naturalis Biodiversity Center, Leiden, The Netherlands

Keywords
cranium; development; function; Partial least squares; allometry; Natricinae; ophidia; 3D geometric morphometrics.

Correspondence
Marko Andjelković, Institute for Biological Research "Siniša Stanković", University of Belgrade, Bulevar Despota Stefana 142, Belgrade 11000, Serbia. Tel:+381112078300; Fax: +381112761433
Email: marko.andjelkovic@ibiss.bg.ac.rs

Editor: Mark-Oliver Rödel

Received 1 February 2017; revised 20 April 2017; accepted 21 April 2017

doi:10.1111/jzo.12477

Abstract

Morphological integration, the covariation among phenotypic traits generated by common development and function, has been in the scope of evolutionary research for decades. As a morphological structure with complex development and various functions, the cranial skeleton represents a particularly interesting model for studies on morphological integration. However, most of the empirical investigations were done on akinetic and compact cranial skeletons of mammals. Here, we explore the pattern of integration in the extremely kinetic cranial skeleton of two closely related snake species, *Natrix natrix* and *N. tessellata* (Natricinae, Colubridae). In snakes, elements of jaws and palates on the left and right side are not spatially connected or firmly fused, allowing independent motion. Spatial independence of skeletal elements on the left and right side and their functional interconnections with extreme kinetic abilities, provide unique feeding performance in this group of tetrapods. By comparing patterns of symmetric and asymmetric components of variation we analysed cavariation patterns between kinetic and akinetic cranial elements. We tested whether the functionally and spatially connected bones are more integrated than disconnected ones and we examine impact of development and function on the morphological integration. We also explored whether and how allometry affects morphological integration in the snake's skull. Using micro-CT scanning 3D geometric morphometrics we showed strong covariation between the braincase and elements of the feeding apparatus, and that spatially disconnected elements are not more integrated than the connected ones. We also showed that function is the main factor that generates the pattern of morphological integration, because the signal of developmental integration is very weak and probably masked by strong functional integration of skeletal elements. Allometry has a significant impact on the morphological integration, by increasing integration of the skull, particularly integration of the lower jaw bones (compound and dentary), prefrontal, palatine and quadrate with the other skeletal elements.

Introduction

Morphological integration, i.e. patterns and intensity of covariation among traits generated by common development and/or function (Olson & Miller, 1958), is considered the principal factor in morphological evolution (Cheverud, 1982, 1996; Klingenberg & Zaklan, 2000; Goswami, 2006a; Kulemeyer *et al.*, 2009; Cooper *et al.*, 2011; Klingenberg, 2013; Labonne *et al.*, 2014). Patterns and intensity of covariation among traits can be described by two not exclusive properties of morphological entities – modularity and morphological integration. Both could be linked to various processes that produce morphological variation and they have an impact on the covariance structure among morphological traits (Cheverud, 1996; Wagner, 1996; Mitteroecker, 2009; Porto *et al.*, 2009). During ontogeny, patterns created by processes generating covariation at early ontogenetic stages may be overwritten and obscured by other processes shaping covariation between structures at later stages (Hallgrímsson *et al.*, 2007). However, in most empirical studies, the influences of developmental and functional integration were considered as major covariance generating factors (Zelditch & Carmichael, 1989; Klingenberg & McIntyre, 1998; Willmore *et al.*, 2005; Breuker, Patterson & Klingenberg, 2006; Ivanović & Kalezić, 2010).

Functional integration - resulting from interactions due to the same organismal function - (Cheverud, 1996) and developmental integration - resulting from interactions of developmental pathways that produce the traits - are often closely related. The match between functional and developmental integration may arise from function-induced growth, building

developmental integration into the functional system (Zelditch, Wood & Swiderski, 2009) or through biomechanical remodelling, such as bone remodelling in response to mechanical load (Klingenberg, 2010). The geometric morphometric approach and implementation of analyses of individual variation in studies of morphological integration and modularity (Klingenberg & Zaklan, 2000) have provided new insight into covariance-generating processes and the possibility to decipher developmental and functional integration as sources of observed morphological integration (Laffont *et al.*, 2009; Ivanović & Kalezić, 2010; Jojić, Blagojević & Vujošević, 2011, 2012).

As a composite morphological structure, with complex development and multiple functional roles, the cranial skeleton represents a challenging model for studies of modularity and integration. Some of the first empirical evaluations of morphological integration were done on the mammalian skull (Cheverud, 1982, 1988). After Cheverud's pioneering investigations, many others studied morphological integration on akinetic cranial skeletons of mammals (Cheverud, 1996; Marroig & Cheverud, 2001; Goswami, 2006b; Mitteroecker & Bookstein, 2008). There are a few studies on partially kinetic avian skulls (Marugán-Lobón & Buscalioni, 2006; Kulemeyer *et al.*, 2009) and the lizard skull (Monteiro & Abe, 1997; Sanger *et al.*, 2012), but, to our knowledge, none on the highly kinetic skull of snakes.

The snake cranium (Fig. 1a) consists of a rigid unit braincase (frontals, postfrontals, parietals, parasphenoid, basisphenoid, basioccipital, supraoccipital, exoccipitals, opisthotics and prootics) and movably connected ones: prefrontals, the snout complex (premaxillae, nasals, septomaxillae and vomers), the upper jaw (maxillae, palatines, pterygoids and ectopterygoids) and the lower jaw (dentaries, splenials, angulars and compound bones) (Rieppel, 1980, 2007; Dwyer & Kaiser, 1997). In snakes, the elements of jaws and palates on the left and right side are not firmly fused (Fig. 1) allowing independent movements (Kardong, 1977, 1979; Cundall & Gans, 1979). Skeletal elements on the same side of the skull are functionally interconnected providing extreme kinetic abilities and feeding performances. Mobility of quadrate bones significantly contributes to the mentioned phenomena. Lower degree of mobility characterize connections: braincase-supratemporals, braincase-prefrontals, dentary-compound.

Such unique structural organization among amniotes, requires different degrees of coordination among skull components and shifts in the pattern of skull integration. The aims of this study are: analysing covariation patterns between kinetic and akinetic cranial elements; testing hypothesis: that functionally and spatially connected bones are more integrated than disconnected ones; determining the impact of development and function on the morphological integration; and exploring whether and how allometry affects morphological integration in the snake's skull.

Materials and methods

Analysed samples

For this study we used 66 alcohol-preserved adult specimens of *N. natrix* ($n = 25$) and *N. tessellata* ($n = 41$), initially collected for ecotoxicological studies (approved by the Serbian Ministry of Energy, Development and Environmental Protection, Permissions Nos: 353-01-640/2012-03 and 353-01-77/2013-08) or killed (trampled on roads, drowned in fishing nets) at the localities of Pančevački rit (Serbia), Obedska bara (Serbia) and Golem Grad Island (FYR of Macedonia). Sex and reproductive maturity were determined from the morphology of the gonads. The grass snake, *Natrix natrix* (Linnaeus, 1758) and the dice snake, *N. tessellata* (Laurenti, 1768) are sister species (Guicking *et al.*, 2006) with similar ecological but different diet preferences (Luiselli & Rugiero, 1991; Mebert, 2011). Specimens were scanned with a micro-CT scanner; Skyscan, Aartselaar, Belgium, at Naturalis Biodiversity Center, The Netherlands (for precise settings see Andjelković, Tomović & Ivanović, 2016) and the 3D surface models of the cranial skeleton were produced using a SkyScan CT Analyser, version 1.10, at a resolution of 26.3 μm.

Data

Landmarks were placed on 3D models of the skull with the Landmark v3.0 software (Wiley *et al.*, 2005). The braincase and each movable skeletal element were digitized separately. For structures with object symmetry, landmarks were scored on both sides. For structures with matching symmetry, landmarks were scored on the left and right copy separately (for detailed description of landmarks see Appendix S1). Each landmark configuration was digitized twice to estimate measurement error (Klingenberg & McIntyre, 1998). Shape variables were extracted using the generalized Procrustes superimposition, for each structure separately (Rohlf & Slice, 1990).

Statistical analyses

As preliminary analyses, we compared covariance matrices between species for each skeletal element. These results showed that species share the same covariance matrices ($P < 0.01$, against null hypothesis of complete dissimilarity for all matrix comparisons). Therefore, we pooled within-species covariance matrix for the analyses of morphological integration. We performed Procrustes ANOVA (Klingenberg & McIntyre, 1998) to examine the level and direction of shape differences for elements on the left and the right side of the skull and to extract symmetric and asymmetric components of shape variance. For the cranial structures with matching asymmetry (Fig. 1a), which are spatially disconnected, independent copies of the same structure on the left and right side, the symmetric component was calculated as the average shape of the structure on the left and right side, while the asymmetric component of shape variance represents differences in shape between the left and right side. For the structures with object symmetry, the symmetric component represents the average shape of the structure and its mirror image, while the asymmetric component reveals the differences between the structure and its mirror image. By using Procrustes ANOVA we estimated among-individual variation, side effect (directional asymmetry), individual-by-side interaction (fluctuating asymmetry) and the effect of measurement error. Strong among-

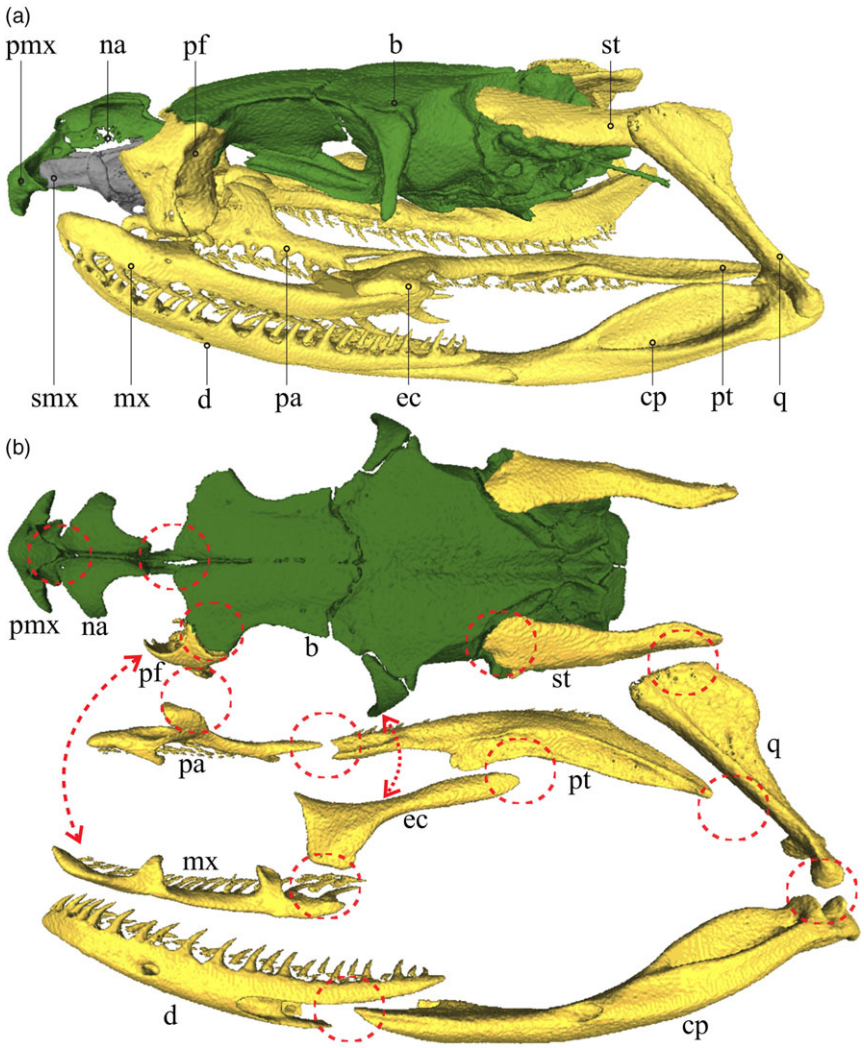

Figure 1 Cranial elements of the *N. natrix* skull; structures with object symmetry are dark grey (green online); pmx - premaxilla, na - nasal, b – braincase), structures with matching symmetry are white (yellow online); pa – palatine, pt - pterygoid, ec - ectopterygoid, mx - maxilla, st – supratemporal, q – quadrate, cp - compound bone, d – dentary and pf – prefrontal). Light grey structures (smx – septomaxillae and vomers) were not analysed. (a) Dorsolateral view of 3D skull model, (b) schematic view of mobile connections between the skeletal elements marked with circles and arrows.

individual covariation in the shape of skull elements would indicate their functional integration, while correlated asymmetries of different skull elements would indicate interactions between developmental pathways (Klingenberg, 2003).

We used Partial least squares (PLS) to quantify the degree of covariation between cranial elements (Rohlf & Corti, 2000; Mitteroecker & Bookstein, 2008; Klingenberg, 2013). We calculated pooled within-group covariance matrices (Mitteroecker & Bookstein, 2008; Klingenberg, 2009) to correct for species and sex effects in skull shape of *Natrix* species (Andjelković *et al.*, 2016). We corrected for the effect of sexual dimorphism because females and males significantly diverge in shape in almost all analysed cranial elements, except for the premaxilla, pterygoid, supratemporal and quadrate bone in *N. natrix*, and the nasal, ectopterygoid and compound bone in *N. tessellata* (Appendix S2). The results of the multivariate regression analyses revealed that a relatively large portion of variance in shape is caused by allometric changes. In the allometry corrected data, sexual shape dimorphism is only observed in the prefrontal of *N. natrix*, and in the premaxilla, braincase, ectopterygoid and maxilla of *N. tessellata*. Covariation between skeletal elements was quantified using the RV coefficients (Escoufier, 1973). The RV coefficient quantifies the total covariation as the sum of all squared covariances between two landmark configurations and gives the strength of association between two sets of variables (Mitteroecker & Bookstein, 2008; Klingenberg, 2013). The significance of RV coefficients is evaluated by a permutation test with 10 000 iterations against the null hypothesis of complete independence between the skeletal elements compared (Klingenberg, 2011). RV

ranges from zero to one. A zero value indicates that the two sets of variables are completely uncorrelated and the value one that structures have the same pattern of variability (Klingenberg, 2009; Laffont *et al.*, 2009). The statistical data from multiple comparisons were adjusted by Bonferroni correction.

To estimate the allometric component of shape variation we performed multivariate regression of shape data (symmetric and asymmetric component) on the centroid size (Monteiro, 1999). Residuals from these multivariate regressions represent allometry-corrected shape variables, and all analyses were repeated on these data. All analyses were performed in MorphoJ (Klingenberg, 2011).

Results

Procrustes ANOVA showed significant directional and fluctuating asymmetry in all skull elements (Table 1). We assessed measurement error from Procrustes ANOVA by comparing the MS error with the MS individual-by-side interaction. Measurement error values were several times lower than those for individual-by-side interactions (Table 1).

Within the skull, the highest RV coefficients was recorded for spatially disconnected structures with matching symmetry (Appendix S3 and S4).

Symmetric component of variation

We detected no statistically significant covariation between nasals and pterygoids and other skeletal elements. Weak covariation was found for premaxillae and supratemporals, while there was significant covariation between all other elements (Fig. 2, Appendix S3). The shape changes associated to covariation between cranial elements for the symmetric component of variation are presented in Fig. 3 and as interactive 3D models (Appendix S5), showing changes from the lowest to the highest scores along PLS1. In covariation with palatine (Fig. 3d1) and ectopterygoid (Fig. 3e1), premaxillae displayed similar shape changes involving shortening and widening of the anterior part and shorter processes. Shortening and increasing the height of the posteroventral parts of premaxilla were characteristics of covariation with the palatine, while elongation and height reduction of the posterior part characterized covariation with the ectopterygoid (Fig. 3a1,a2). Shape changes of the braincase relative to maxilla (Fig. 3f1), ectopterygoid (Fig. 3e2), quadrate (Fig. 3h1), compound (Fig. 3i1) and dentary (Fig. 3j1) had a similar pattern (Fig. 3b1–b5) and corresponded to widening of the anterior and medial part of the braincase and narrowing of its posterior part. A different pattern was found relative to the prefrontal (Fig. 3c1) and palatine (Fig. 3d2). This was related to shortening and narrowing of the anterior part, widening of the medial and posterior parts, shortening of the posterior part, and lengthening and narrowing of the postfrontal (Fig. 3b6,b7). Prefrontal shape changes relative to the braincase (Fig. 3b6), palatine (Fig. 3d3) and maxilla (Fig. 3f5) involved shortening, widening and increasing the height of the entire structure (Fig. 3c1–c3); while shape changes relative to the ectopterygoid (Fig. 3e3), quadrate (Fig. 3h2) and dentary (Fig. 3j2) included elongation and reduction of the height (Fig. 3c4–c6). The palatine showed similar shape changes in covariation with premaxilla (Fig. 3a1), braincase (Fig. 3b7), prefrontal (Fig. 3c2), maxilla (Fig. 3f6) and compound (Fig. 3i5). This included narrowing and dorsoventral flattening, shortening of the anterior and elongation of the posterior part (Fig. 2d1–d5). In covariation with the ectopterygoid (Fig. 3e4), shape changes were expressed as widening of the palatine, enhancement of its curvature in the anteroposterior direction, and shortening of the anterior part (Fig. 2d6). The shape changes of the ectopterygoid relative to the premaxilla (Fig. 3a2), braincase (Fig. 3b1), prefrontal (Fig. 3 c4), palatine (Fig. 3d6), maxilla (Fig. 3f2), compound bone (Fig. 3i3) and dentary (Fig. 3j3) involved narrowing of the entire structure and increased curvature of its anterior part (Fig. 3e1–e7). Maxilla shape changes, relative to the braincase (Fig. 3b2), ectopterygoid (Fig. 3e5), quadrate (Fig. 3h3) and dentary (Fig. 3j4), included elongation of the entire structure, widening of the palatine and ectopterygoid processes, and enhancement of the curvature in the anteroposterior

Table 1 Procrustes ANOVAs of skull structure shape. Statistically significant side effects represent the significance of directional asymmetry, while individual × side interactions represent the significance of fluctuating asymmetry

	Individual				Side				Individual × Side				Error 1	
	ms	d.f.	*F*	*P*	ms	d.f.	*F*	*P*	ms	d.f.	*F*	*P*	ms	d.f.
Premaxilla	0.003315	585	31.98	0.0001	0.000353	8	3.41	0.0008	0.000104	520	2.97	0.0001	0.000035	969
Nasal	0.002742	520	21.39	0.0001	0.000324	9	2.53	0.0075	0.000128	585	3.35	0.0001	0.000038	952
Braincase	0.000083	4355	15.94	0.0001	0.000019	61	3.63	0.0001	0.000005	3965	4.75	0.0001	0.000001	8448
Prefrontal	0.001898	1280	8.10	0.0001	0.002233	20	9.54	0.0001	0.000234	1280	3.48	0.0001	0.000067	2600
Palatine	0.004421	910	47.58	0.0001	0.000366	14	3.94	0.0001	0.000093	910	6.80	0.0001	0.000014	1848
Pterygoid	0.001431	1088	18.54	0.0001	0.000471	17	6.10	0.0001	0.000077	1088	5.39	0.0001	0.000014	2210
Ectopterygoid	0.001450	910	12.63	0.0001	0.000635	14	5.53	0.0001	0.000115	910	4.26	0.0001	0.000027	1848
Maxilla	0.000418	2275	10.62	0.0001	0.000473	35	12.03	0.0001	0.000039	2275	2.56	0.0001	0.000015	4620
Supratemporal	0.001393	520	10.88	0.0001	0.003234	8	25.28	0.0001	0.000128	520	3.07	0.0001	0.000042	1056
Quadrate	0.001991	704	20.71	0.0001	0.000340	11	3.54	0.0001	0.000096	704	7.39	0.0001	0.000013	1430
Compound	0.000338	1612	9.94	0.0001	0.000112	26	3.31	0.0001	0.000034	1612	2.49	0.0001	0.000014	3276
Dentary	0.001128	910	6.22	0.0001	0.002197	14	12.12	0.0001	0.000181	910	6.38	0.0001	0.000028	1848

(a)

	1.	2.	3.	4.	5.	6.	7.	8.	9.	10.	11.	12.
1. Premaxilla												
2. Nasal												
3. Braincase				*					*			
4. Prefrontal			*	*								
5. Palatine	*		*	*	*							
6. Pterygoid						*						
7. Ectopterygoid	*		*	*	*		*					
8. Maxilla			*	*	*		*	*				
9. Supratemporal									*			
10. Quadrate			*	*				*	*	*		
11. Compound			*		*		*			*	*	
12. Dentary			*	*			*	*		*		*

(b)

	1.	2.	3.	4.	5.	6.	7.	8.	9.	10.	11.	12.
1. Premaxilla												
2. Nasal												
3. Braincase				*					*			
4. Prefrontal			*	*								
5. Palatine					*							
6. Pterygoid						*						
7. Ectopterygoid	*		*	*		*	*					
8. Maxilla			*		*		*	*				
9. Supratemporal			*						*			
10. Quadrate								*	*	*		
11. Compound							*				*	
12. Dentary			*					*				*

Figure 2 The strength of covariation between skeletal elements in the *Natrix* skull expressed as RV coefficients for (a) allometric and (b) non-allometric components of shape variation. Symmetric component of shape variation – bottom left to the diagonal; asymmetric component of shape variation – top right to the diagonal. Covariation between left and right side of structures with matching symmetry – on the diagonal. The cells referring to the skeletal elements of the feeding apparatus that are spatially connected are shaded. Statistically significant RV coefficients (after Bonferroni corrections) are marked by an asterisk.

direction (Fig. 3f1–f4). A different pattern of shape changes was found relative to the prefrontal (Fig. 3c3) and palatine (Fig. 3d4), and these shape changes involved shortening and narrowing of the entire structure, narrowing but widening the distance between the processes (Fig. 3f5–f6). Supratemporal shape changes, relative to the quadrate (Fig. 3h6) were expressed as augmentation of the volume of the entire structure and shortening of its posterior part (Fig. 3g1). Similar shape changes of the quadrate in covariation with braincase (Fig. 3b3), prefrontal (Fig. 3c5), maxilla (Fig. 3f3), compound (Fig. 3i2) and dentary (Fig. 3j5) involved narrowing and elongation of the entire structure (Fig. 3h1–h5). In covariation with the supratemporal (Fig. 3g1) shape changes of the quadrate bone corresponded to shortening of its anterodorsal and ventrolateral parts and elongation of the posterodorsal and ventromedial parts (Fig. 3h6). Shape changes of the compound bone, relative to the braincase (Fig. 3b4) and quadrate (Fig. 3h4), were expressed as shortening, flattening and increase in height, as well as positioning of its articular surface with the quadrate more posteriorly (Fig. 3i1,i2). In covariation with the ectopterygoid (Fig. 3e6) and dentary (Fig. 3j6) shape changes were marked by height reduction (Fig. 3i3,i4), while in covariation with the palatine (Fig. 3d5) shape changes involved elongation and widening of the entire structure, increased height of the surangular crest and positioning the articular surface with the quadrate more anteriorly (Fig. 3i5). Shape changes of the dentary in covariation with the braincase (Fig. 3b5), prefrontal (Fig. 3c6), ectopterygoid (Fig. 3e7), maxilla (Fig. 3f4), quadrate (Fig. 3h5) and compound bone (Fig. 3i4), included widening of the anterior, narrowing of the medial, shortening of the posterodorsal and elongation of the posteroventral part, as well as curvature reduction in the anteroposterior direction (Fig. 3j1–j6).

Asymmetric component of variation

Statistically significant RV coefficients were found between the braincase and prefrontals and braincase and supratemporals, only (Fig. 2, Appendix S3).

Allometry

Significant static allometry was confirmed for all analysed structures, except for the premaxilla (Appendix S6). PLS analyses on allometry-corrected data showed marked reduction in the number of statistically significant covariations between skeletal elements, except for braincase, ectopterygoid and maxilla (Fig. 2b, Appendix S4). The number of significant correlations for palate, quadrate and lower jaw bones (dentary and compound) with other skeletal elements was three times lower for the allometry-corrected compared to the allometry-included dataset (Fig. 2).

The shape changes associated to covariation between cranial elements for allometry-corrected data are presented in Fig. 4 and Appendix S7. Shape changes of the ectopterygoid in covariation with other elements were similar to those described for allometry included data, but were substantially different for covariation between the maxilla and dentary with other skeletal elements. Maxilla shape changes relative to the braincase (Fig. 4b1), palatine (Fig. 4d1), quadrate (Fig. 4i1) and dentary (Fig. 4k2) were expressed as shortening and widening of its anterior part, elongation of the posterior part and palatine process, shortening and widening of the ectopterygoid process, and positioning of both processes more anteriorly (Fig. 4g1–g4). Associated shape changes of the braincase involved narrowing and shortening of the anterior part, widening of the medial part, widening and elongation of the posterior part

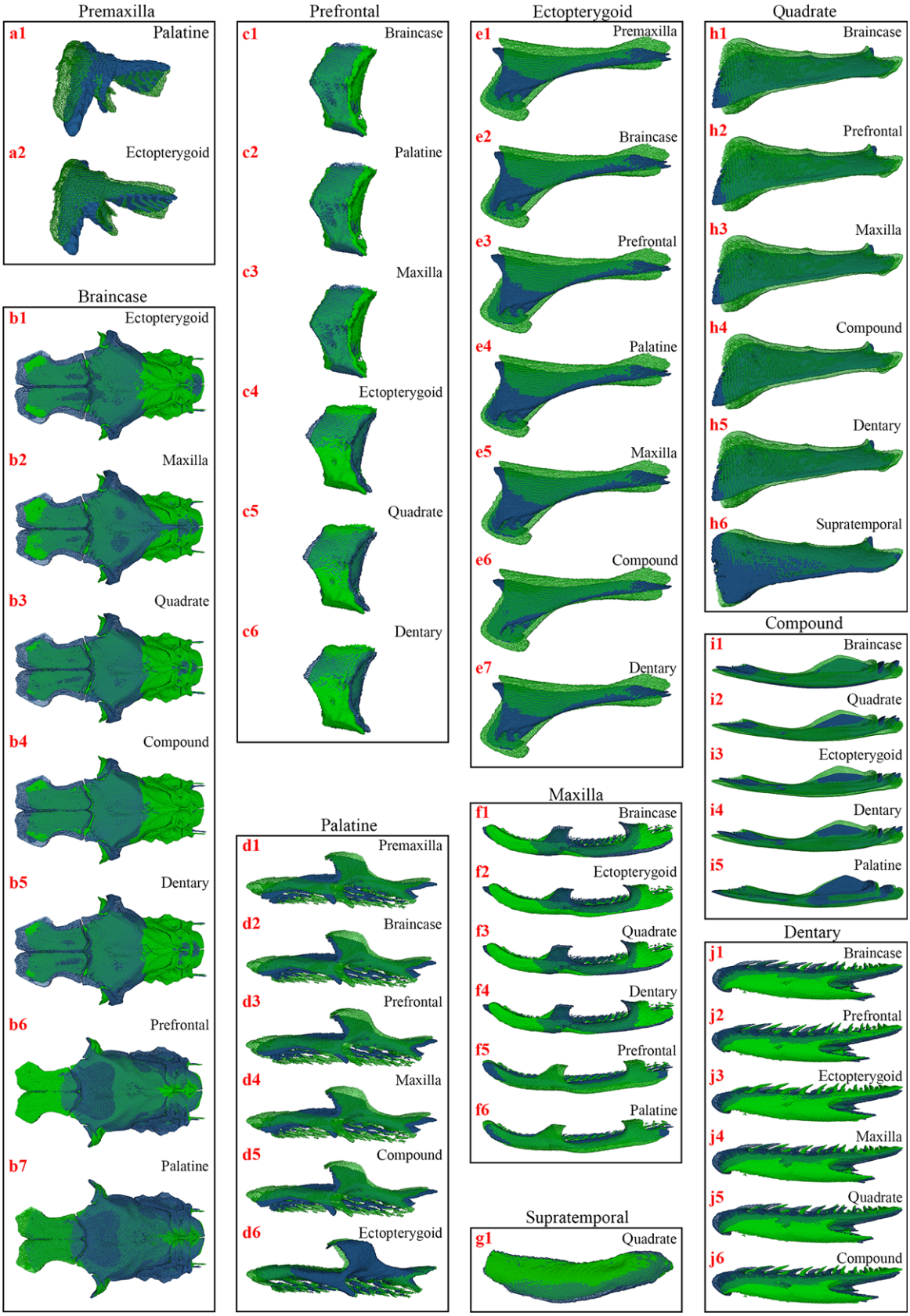
Premaxilla
a1 Palatine
a2 Ectopterygoid
Braincase
b1 Ectopterygoid
b2 Maxilla
b3 Quadrate
b4 Compound
b5 Dentary
b6 Prefrontal
b7 Palatine
Prefrontal
c1 Braincase
c2 Palatine
c3 Maxilla
c4 Ectopterygoid
c5 Quadrate
c6 Dentary
Palatine
d1 Premaxilla
d2 Braincase
d3 Prefrontal
d4 Maxilla
d5 Compound
d6 Ectopterygoid
Ectopterygoid
e1 Premaxilla
e2 Braincase
e3 Prefrontal
e4 Palatine
e5 Maxilla
e6 Compound
e7 Dentary
Maxilla
f1 Braincase
f2 Ectopterygoid
f3 Quadrate
f4 Dentary
f5 Prefrontal
f6 Palatine
Supratemporal
g1 Quadrate
Quadrate
h1 Braincase
h2 Prefrontal
h3 Maxilla
h4 Compound
h5 Dentary
h6 Supratemporal
Compound
i1 Braincase
i2 Quadrate
i3 Ectopterygoid
i4 Dentary
i5 Palatine
Dentary
j1 Braincase
j2 Prefrontal
j3 Ectopterygoid
j4 Maxilla
j5 Quadrate
j6 Compound

Figure 3 Picture of combined 3D models showing shape changes along the PLS1 axis: light grey (green online) represents a shape related to the negative end, while dark grey (blue online) represents a shape at the positive end of the axis. The pictures of the combined model show the dorsal projection of the braincase, the left maxilla and ectopterygoid, lateral projection of the premaxilla, the left prefrontal, palatine, quadrate, compound bones, dentary and supratemporal. PLS was performed on the allometric component of shape variation. (Elements are not shown in real scale).

(Fig. 4b1). Associated shape changes of the palatine included flattening and an increase in height (Fig. 4d1). Concerning the quadrate, alterations included widening of its dorsal part, shortening of the ventrolateral and elongation of the ventromedial part of this bone (Fig. 4i1). Related shape changes of the dentary included height augmentation and flattening of the anterior part, elongation of the posterodorsal part and shortening of the posteroventral part (Fig. 4k2). In covariation with the ectopterygoid, shape changes of the maxilla included elongation and narrowing of the anterior part, shortening and narrowing of the posterior part and shortening and narrowing of both maxillary processes (Fig. 4g5). Both dentary and braincase structures exhibited similar covariation to those previously described for covariation with the maxilla (Fig. 4b1,b2, k1,k2).

Discussion

Compared to other amniote groups with largely compact skulls, the skeletal elements of the upper jaw and palates of snakes are separated from the braincase and joined into linked chains allowing extreme motion relative to the braincase (Kardong, 1977, 1979). The series of linked bones on the left and right side (prefrontals, maxillae, palatines, pterygoids, ectopterygoids, supratemporals, quadrates, compound bones and dentaries) are spatially independent cranial elements with matching symmetry. As expected, the highest covariation was recorded between these paired structures with matching symmetry, which share the same genetic basis, developmental programs and functions (Labonne *et al.*, 2014).

Generally, functionally correlated traits display a higher level of correlation than functionally independent ones (Cooper *et al.*, 2011). Concerning morphological integration of the cranial skeleton, functional integration due to biomechanical requirements in feeding has been documented in mammals (Hallgrímsson *et al.*, 2004; Monteiro, Bonato & Dos Reis, 2005; Drake & Klingenberg, 2010). In this group, the face and the braincase display modular separation despite strong integration of the entire skull (Bookstein *et al.*, 2003; Bastir & Rosas, 2006; Mitteroecker & Bookstein, 2008; Singh *et al.*, 2012). In *Natrix* snakes, there is a high level of morphological integration between the braincase and elements of the feeding apparatus, while the snout elements (premaxillae and nasals) express the lowest degree of correlation with other skeletal elements. Unexpectedly, the supratemporals and pterygoids, which are part of the functional chain of the feeding apparatus, showed low covariation with other functionally linked bones. The high level of integration between the compact and akinetic braincase with elements of the feeding apparatus may be an adaptation for optimal capture and ingestion of prey, thus preventing mechanical injuries to the sense organs and brain. On the other hand, the lower functional integration of snout elements could be explained by their minor role in feeding. Weak functional integration of the pterygoid is not expected because this bone has a major role in transporting prey through the oral cavity (Cundall & Greene, 2000). A possible explanation for this low integration could be that its functional optimization and surrounding connections with muscles and ligaments constrain close integration.

Significant developmental integration was observed in the cranial skeleton in mammals (Zelditch & Carmichael, 1989; Hallgrímsson *et al.*, 2004). However, in *Natrix* snakes, developmental integration was only detected between the braincase and prefrontals and between the braincase and supratemporals. Both prefrontals and supratemporals are tightly connected to the braincase by fibrous connective tissue. They provide suspensory support to the jaws and palate and connect them to the braincase. Both skeletal elements with limited kinesis are included in the linked chain of movable elements (Kardong, 1977, 1979). The absence of significant covariation for the asymmetric component for all other movable skull elements could be the result of strong functional integration which masks or "overwrites" other covariation-generating processes, including developmental ones (Hallgrímsson *et al.*, 2009).

In most studies of modularity and morphological integration, spatial contingency is regarded as a prerequisite for both developmental and functional tissue-tissue interactions covariation (Jojić *et al.*, 2007; Ivanović & Kalezić, 2010; Sanger *et al.*, 2012; Labonne *et al.*, 2014), so phenotypic covariance cannot be interpreted without reference to their spatial and geometric dependencies (Mitteroecker, 2009). Our assumption that functionally and spatially (mechanically) connected bones would be more integrated than spatially disconnected ones was not supported by the observed covariation among skeletal elements. Contrary to our expectation, the number of significant covariations between spatially connected cranial elements was less than half that between spatially disconnected ones. Such results could be due to the fact that we considered only direct articulations or ligamentous connections between the skeletal elements. In many empirical studies of morphological integration (Cheverud, 1982, 1988, 1996; Ackermann, 2005; Goswami, 2006b) muscle insertions and bone soft-tissue interactions were considered as the main epigenetic factors producing functional integration of the mammalian skull. Therefore, soft tissue interactions could underlie the observed high covariation between spatially disconnected bones.

Size related changes in shape during an organism's growth are crucial for the organization of the phenotype and establishment of adult body proportions. Allometry is regarded as one of the dominant factors of morphological integration (Zelditch & Fink, 1995; Klingenberg, 2009, 2013). In the analysed *Natrix* snakes, allometry markedly increased the strength of covariation between cranial elements. However, the impact of allometry was not consistent, as for some structures it increased while for

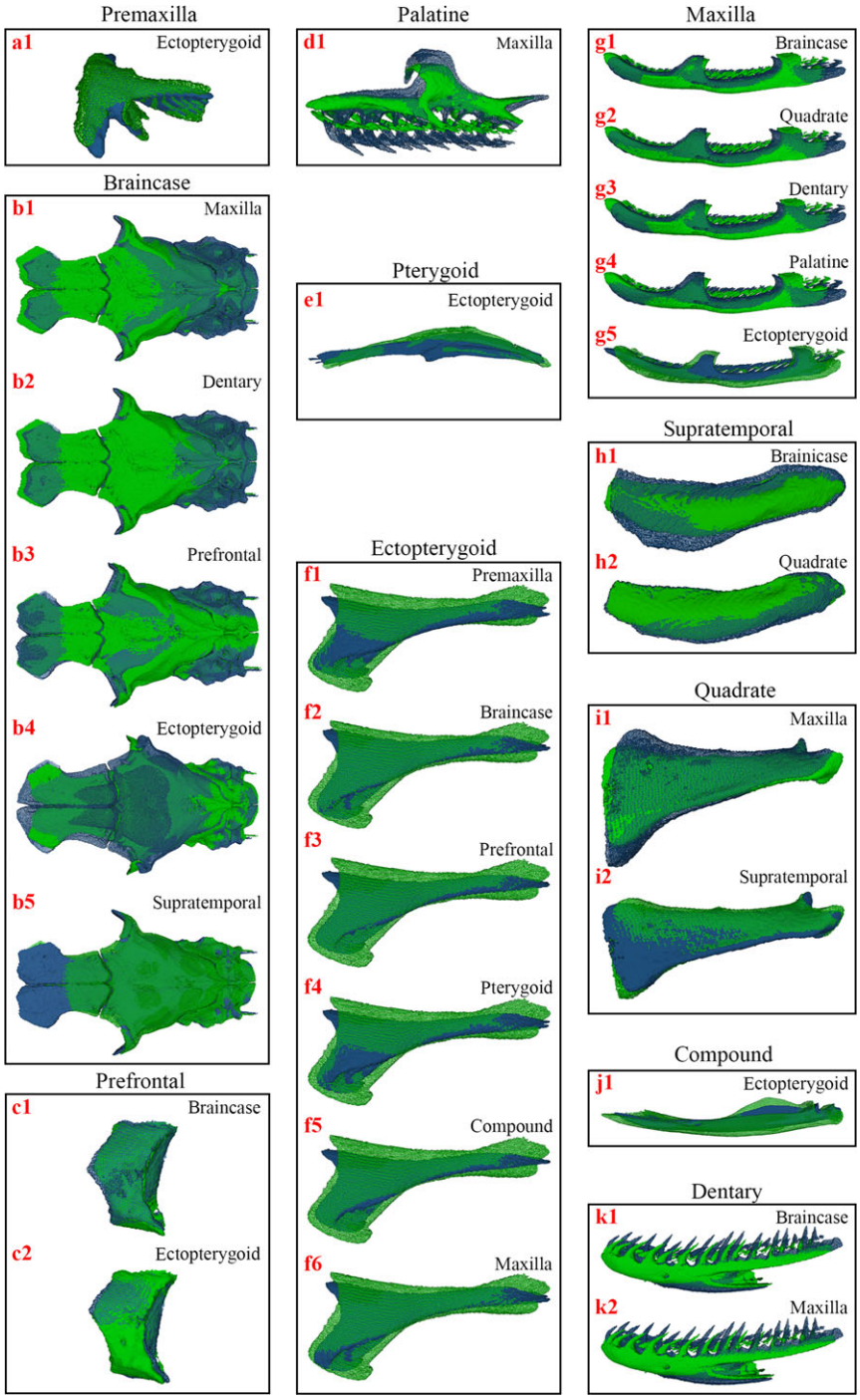

Figure 4 Picture of combined 3D models showing shape changes along the PLS1 axis: light grey (green online) represents a shape related to the negative end, while dark grey (blue online) represents a shape at the positive end of the axis. The pictures of the combined model show the dorsal projection of the braincase, the left maxilla, pterygoid and ectopterygoid, lateral projection of the premaxilla, the left prefrontal, palatine, quadrate, compound bones, dentary and supratemporal. PLS was performed on the non-allometric component of shape variation. (Elements are not shown in real scale).

others it had a small or no effect on morphological integration (Fig. 2). For example, allometry largely contributed to integration of the palatine, quadrate and the lower jaw bones (dentary and compound) with other skull elements. The number of significant covariations among these and other skull bones for allometry-included data was threefold the number of correlations for allometry-corrected data. The shape changes for allometry-corrected data largely coincided with allometry-included ones, with the exception of maxilla and dentary. The observed covariations among skeletal elements could not be clearly related to their spatial or functional connections (Fig. 2). However, the significant influence of allometric shape changes on covariation between the lower jaw bones, quadrate and palatine with the other skull parts could be crucial for their coordinated changes in terms of function, in both space and time.

The observed covariation patterns indicate that morphological integration of the cranial skeleton in *Natrix* snakes is largely influenced by functional constraints and allometric shape changes, particularly by allometric changes of the visceral part of the cranial skeleton. Future research on larger datasets is needed to explore how different dietary preferences or environmental requirements have an impact on morphological integration of the kinetic skull and whether strong functional integration between elements of the feeding apparatus and braincase can limit or direct morphological changes in snakes.

Acknowledgements

We thank Christian Klingenbreg for suggestions regarding data analyses and two anonymous reviewers for comments on a previous version of the manuscript. This research was financed by the Ministry of Education, Science and Technological Development of the Republic of Serbia (Grant No. 173007 and 173043). AI acknowledges grants from SyntheSys (NL-TAF 1245, NL-TAF 3082) and a Naturalis Biodiversity Center 'Temminck fellowship'.

References

Ackermann, R.R. (2005). Ontogenetic integration of the hominoid face. *J. Hum. Evol.* **48**, 175–197.

Andjelković, M., Tomović, L. & Ivanović, A. (2016). Variation in skull size and shape of two snake species (*Natrix natrix* and *Natrix tessellata*). *Zoomorphology* **135**, 243–253.

Bastir, M. & Rosas, A. (2006). Correlated variation between the lateral basicranium and the face: a geometric morphometric study in different human groups. *Arch. Oral Biol.* **51**, 814–824.

Bookstein, F.L., Gunz, P., Mitteroecker, P., Prossinger, H., Schaeer, K. & Seidler, H. (2003). Cranial integration in Homo: singular warps analysis of the midsagittal plane in ontogeny and evolution. *J. Hum. Evol.* **44**, 167–187.

Breuker, C.J., Patterson, J.S. & Klingenberg, C.P. (2006). A single basis for developmental buffering of Drosophila wing shape. *PLoS ONE* **1**, e7.

Cheverud, J.M. (1982). Phenotypic, genetic, and environmental morphological integration in the cranium. *Evolution* **36**, 499–516.

Cheverud, J.M. (1988). Spatial-analysis in morphology illustrated by rhesus macaque cranial growth and integration. *Am. J. Phys. Anthropol.* **75**, 195–196.

Cheverud, J.M. (1996). Developmental integration and the evolution of pleiotropy. *Am. Zool.* **36**, 44–50.

Cooper, W.J., Wernle, J., Mann, K. & Albertson, R.C. (2011). Functional and genetic integration in the skulls of Lake Malawi cichlids. *Evol. Biol.* **38**, 316–334.

Cundall, D. & Gans, C. (1979). Feeding in water snakes: an electromyographic study. *J. Exp. Zool.* **209**, 189–207.

Cundall, D. & Greene, H.W. (2000). Feeding in snakes. In *Feeding: form, function, and evolution in Tetrapod vertebrates*: 293–333. Schwenk, K. (Ed). San Diego, CA: Academic Press.

Drake, A.G. & Klingenberg, C.P. (2010). Large-scale diversification of skull shape in domestic dogs: disparity and modularity. *Am. Nat.* **175**, 289–301.

Dwyer, C.M. & Kaiser, H. (1997). Relationship between skull form and prey selection in the thamnophiine snake genera *Nerodia* and *Regina*. *J. Herpetol.* **31**, 463–475.

Escoufier, Y. (1973). Le traitement des variables vectorielles. *Biometrics* **29**, 751–760.

Goswami, A. (2006a). Cranial modularity shifts during mammalian evolution. *Am. Nat.* **168**, 270–280.

Goswami, A. (2006b). Morphological integration in the carnivoran skull. *Evolution* **60**, 169–183.

Guicking, D., Lawson, R., Joger, U. & Wink, M. (2006). Evolution and phylogeny of the genus *Natrix* (Serpentes: Colubridae). *Biol. J. Linn. Soc.* **87**, 127–143.

Hallgrímsson, B., Willmore, K., Dorval, C. & Cooper, D.M. (2004). Craniofacial variability and modularity in macaques and mice. *J. Exp. Zoolog. B Mol. Dev. Evol.* **302**, 207–225.

Hallgrímsson, B., Lieberman, D.E., Young, N.M., Parsons, T. & Wat, S. (2007). Evolution of covariance in the mammalian skull. In *Tinkering: the Microevolution of Development*: 164–190. Bock, G. & Goode, J. (Eds.). Chichester: John Wiley.

Hallgrímsson, B., Jamniczky, H., Young, N.M., Rolian, C., Parsons, T.E., Boughner, J.C. & Marcucio, R.S. (2009). Deciphering the palimpsest: studying the relationship between morphological integration and phenotypic covariation. *Evol. Biol.* **36**, 355–376.

Ivanović, A. & Kalezić, M.L. (2010). Testing the hypothesis of morphological integration on a skull of a vertebrate with a biphasic life cycle: a case study of the alpine newt. *J. Exp. Zoolog. B Mol. Dev. Evol.* **314**, 527–538.

Jojić, V., Blagojević, J., Ivanović, A., Bugarski-Stanojević, V. & Vujošević, M. (2007). Morphological integration of the mandible in yellow-necked field mice: the effects of B chromosomes. *J. Mammal.* **88**, 689–695.

Jojić, V., Blagojević, J. & Vujošević, M. (2011). B chromosomes and cranial variability in yellow-necked field mice (Apodemus flavicollis). *J. Mammal.* **92**, 396–406.

Jojić, V., Blagojević, J. & Vujošević, M. (2012). Two-module organization of the mandible in the yellow-necked mouse: a comparison between two different morphometric approaches. *J. Evol. Biol.* **25**, 2489–2500.

Kardong, K.V. (1977). Kinesis of the jaw apparatus during swallowing in the cottonmouth snake, *Agkistrodon piscivorus*. *Copeia* **1977**, 338–348.

Kardong, K.V. (1979). "Protovipers" and the evolution of snake fangs. *Evolution* **33**, 433–443.

Klingenberg, C.P. (2003). Developmental instability as a research tool: using patterns of fluctuating asymmetry to infer the developmental origins of morphological integration. In *Developmental instability: causes and consequences*: 427–442. Polak, M. (Ed.). New York: Oxford University Press.

Klingenberg, C.P. (2009). Morphometric integration and modularity in configurations of landmarks: tools for evaluating a priori hypotheses. *Evol. Dev.* **11**, 405–421.

Klingenberg, C.P. (2010). Evolution and development of shape: integrating quantitative approaches. *Nat. Rev. Genet.* **11**, 623–635.

Klingenberg, C.P. (2011). MorphoJ: an integrated software package for geometric morphometrics. *Mol. Ecol. Resour.* **11**, 353–357.

Klingenberg, C.P. (2013). Cranial integration and modularity: insights into evolution and development from morphometric data. *Hystrix Ital. J. Mammal.* **24**, 43–58.

Klingenberg, C.P. & McIntyre, G.S. (1998). Geometric morphometrics of developmental instability: analyzing patterns of fluctuating asymmetry with procrustes methods. *Evolution* **52**, 1363–1375.

Klingenberg, C.P. & Zaklan, S.D. (2000). Morphological integration between developmental compartments in the Drosophila wing. *Evolution* **54**, 1273–1285.

Kulemeyer, C., Asbahr, K., Gunz, P., Frahnert, S. & Bairlein, F. (2009). Functional morphology and integration of corvid skulls–a 3D geometric morphometric approach. *Front. Zool.* **6**, 2.

Labonne, G., Navarro, N., Laffont, R., Chateau-Smith, C. & Montuire, S. (2014). Developmental integration in a functional unit: deciphering processes from adult dental morphology. *Evol. Dev.* **16**, 224–232.

Laffont, R., Renvoisé, E., Navarro, N., Alibert, P. & Montuire, S. (2009). Morphological modularity and assessment of developmental processes within the vole dental row (*Microtus arvalis*, Arvicolinae, Rodentia). *Evol. Dev.* **11**, 302–311.

Luiselli, L. & Rugiero, L. (1991). Food niche partitioning by water snakes (genus *Natrix*) at a freshwater environment in central Italy. *J. Freshw. Ecol.* **6**, 439–444.

Marroig, G. & Cheverud, J.M. (2001). A comparison of phenotypic variation and covariation patterns and the role of phylogeny, ecology, and ontogeny during cranial evolution of New World monkeys. *Evolution* **55**, 2576–2600.

Marugán-Lobón, J. & Buscalioni, Á.D. (2006). Avian skull morphological evolution: exploring exo-and endocranial covariation with two-block partial least squares. *Zoology* **109**, 217–230.

Mebert, K. (2011). *The dice snake, Natrix tessellata: biology, distribution and conservation of a palaearctic species*. Rheinbach: Mertensiella.

Mitteroecker, P. (2009). The developmental basis of variational modularity: insights from quantitative genetics, morphometrics, and developmental biology. *Evol. Biol.* **36**, 377–385.

Mitteroecker, P. & Bookstein, F. (2008). The evolutionary role of modularity and integration in the hominoid cranium. *Evolution* **62**, 943–958.

Monteiro, L.R. (1999). Multivariate regression models and geometric morphometrics: the search for causal factors in the analysis of shape. *Syst. Biol.* **48**, 192–199.

Monteiro, L.R. & Abe, A.S. (1997). Allometry and morphological integration in the skull of Tupinambis merianae (Lacertilia: Teiidae). *Amphib.-Reptil.* **18**, 397–405.

Monteiro, L.R., Bonato, V. & Dos Reis, S.F. (2005). Evolutionary integration and morphological diversification in complex morphological structures: mandible shape divergence in spiny rats (Rodentia, Echimyidae). *Evol. Dev.* **7**, 429–439.

Olson, E.C. & Miller, R.L. (1958). *Morphological integration*. 1st edn. Chicago: University of Chicago Press.

Porto, A., de Oliveira, F.B., Shirai, L.T., De Conto, V. & Marroig, G. (2009). The evolution of modularity in the mammalian skull I: morphological integration patterns and magnitudes. *Evol. Biol.* **36**, 118–135.

Rieppel, O. (1980). The evolution of the ophidian feeding system. *Zool. Jahrbucher Abt. Anat. Ontog. Tiere* **103**, 551–564.

Rieppel, O. (2007). The naso-frontal joint in snakes as revealed by high-resolution X-ray computed tomography of intact and complete skulls. *Zool. Anz. - J. Comp. Zool.* **246**, 177–191.

Rohlf, F.J. & Corti, M. (2000). Use of two-block partial least-squares to study covariation in shape. *Syst. Biol.* **49**, 740–753.

Rohlf, F.J. & Slice, D. (1990). Extensions of the Procrustes method for the optimal superimposition of landmarks. *Syst. Biol.* **39**, 40–59.

Sanger, T.J., Mahler, D.L., Abzhanov, A. & Losos, J.B. (2012). Roles for modularity and constraint in the evolution of cranial diversity among Anolis lizards. *Evolution* **66**, 1525–1542.

Singh, N., Harvati, K., Hublin, J.-J. & Klingenberg, C.P. (2012). Morphological evolution through integration: a quantitative study of cranial integration in Homo, Pan, Gorilla and Pongo. *J. Hum. Evol.* **62**, 155–164.

Wagner, G.P. (1996). Homologues, natural kinds and the evolution of modularity. *Am. Zool.* **36**, 36–43.

Wiley, D.F., Amenta, N., Alcantara, D., Ghosh, D., Kil, Y.J., Delson, E., Harcourt-Smith, W., Rohlf, F.J., St John, K. and Hamann, B. (2005). Evolutionary morphing. In *Proceedings of IEEE Visualization 2005*: 431–438.

Willmore, K.E., Klingenberg, C.P., Hallgrímsson, B. & Wainwright, P. (2005). The relationship between fluctuating

asymmetry and environmental variance in rhesus macaque skulls. *Evolution* **59**, 898–909.
Zelditch, M.L. & Carmichael, A.C. (1989). Ontogenetic variation in patterns of developmental and functional integration in skulls of Sigmodon fulviventer. *Evolution* **43**, 814–824.
Zelditch, M.L. & Fink, W.L. (1995). Allometry and developmental integration of body growth in a piranha, *Pygocentrus nattereri* (Teleostei: Ostariophysi). *J. Morphol.* **223**, 341–355.
Zelditch, M.L., Wood, A.R. & Swiderski, D.L. (2009). Building developmental integration into functional systems: function-induced integration of mandibular shape. *Evol. Biol.* **36**, 71–87.

Supporting Information

Additional Supporting Information may be found in the online version of this article:

Appendix S1. The list and definition of landmarks scored on premaxilla, nasals, braincase, prefrontal, palatine, pterygoid, ectopterygoid, maxilla, supratemporal, quadrate, compound bones and dentary.
Appendix S2. Sexual dimorphism in shape expressed in units of Procrustes distance (PD) between females and males and statistical significance of differences in shape obtained by permutation test (10 000 iterations) for *N. natrix* and *N. tessellata*. *P* - statistical significance (values highlighted in bold are statistically significant).
Appendix S3. PLS analysis for allometry-included data: RV coefficients for symmetric and asymmetric components of shape variation (below and above the diagonal, respectively). Statistically significant *P* values after Bonferroni correction for multiple comparisons are shaded and bold.
Appendix S4. PLS analysis for allometry-corrected data: RV coefficients for symmetric and asymmetric components of shape variation (below and above the diagonal, respectively). Statistically significant *P* values after Bonferroni correction for multiple comparisons are shaded and bold.
Appendix S5. Shape changes along the PLS1 axis. Green marks a shape related to the negative end, while blue marks a shape on the positive end of the axis. PLS analysis was performed on the allometric component of shape variation.
Appendix S6. Multivariate regression (pooled within species) of shape data (symmetric and asymmetric component) on the centroid size, % - the proportion of variance in shape explained, *P* - statistical significance (values highlighted in bold are statistically significant).
Appendix S7. Shape changes along the PLS1 axis. Green marks a shape related to the negative end, while blue marks a shape on the positive end of the axis. PLS analysis was performed on the non-allometric component of shape variation.